International Journal of
Mathematical Modelling & Computations
Vol. 14, No. 03, Summer 2024, 241- 254
DOI:10.71932/ijm.2024.1194826

Haar Wavelet Method for Numerical Solution of Two-Dimensional Partial Fractional Integro-Differential Equations

Ruhollah Takhtipour[a], Laleh Hooshangian[b,*]

Sara Shokrolahi Yancheshmeh[a], Jafar Esmaily[a]

[a] *Department of Mathematics, Ahvaz Branch, Islamic Azad University, Ahvaz, Iran*;
[b] *Department of Mathematics, Dezful Branch, Islamic Azad University, Dezful, Iran.*

Abstract. This article examines new methods for solving fractional integral differential equations of Fredholm using wavelets. In this research, first, fractional integral differential equations and their special properties are introduced. Then, the importance of using wavelets as a tool for analyzing and solving these equations is explained. Wavelet methods have many advantages due to their ability to display signals and analyze nonlinear and indirect data, especially in complex and dynamic problems. The article describes various algorithms and techniques that, by utilizing the properties of wavelets, can be used to achieve numerical and analytical solutions of the above equations. Convergence results and error evaluation are also presented in this article using examples to demonstrate the effectiveness and high efficiency of wavelet methods in solving fractional integral differential equations of Fredholm. It also reduces the variable-order fractional derivative theorem to a system of algebraic equations by approximating the Haar wavelet and integrating it.

Received: 02 June 2024, Revised: 07 August 2024, Accepted: 19 August 2024.

Keywords: Haar wavelet method; derivative fractional; error analysis; numerical solution; two-dimensional integro-differential equation.

AMS Subject Classification:

Index to information contained in this paper

1. Introduction

Solving partial differential equations has been of interest to scientists for a long time. Many researchers have proposed this method due to the applicability of frac-

*Corresponding author. Email: : l.hooshangian1@gmail.com

tional differential integral equations of singular type [19, 24]. Recently, fractional integral differential equations have been used to model many physical phenomena in various fields of non-linear oscillation of earthquakes, fluid dynamics traffic, continuum, statistical mechanics of signal processing, control theory, dynamics, and the relationship between nanoparticles [9, 21]. Numerous numerical methods have been thoroughly researched to solve these equations, including Fourier transform, Laplace analysis, fractional differential transform, finite difference method, orthogonal functions, Adomian decomposition method, variable iteration method, and homotopy analysis method. They are used to obtain approximate solutions for fractional equations [10, 12, 20].

Fractional integral differential equations are valuable in modeling many phenomena [13, 23]. Over the past four decades, scientists have focused on the theory and applications of partial differential equations of fractional order, which generalize differential equations of the correct order. One such method that has gained attention is the modified homotopy analysis transformation method [15, 17]. Shahsavaran and Babolian computed the numerical value of Fredholm's non-linear integral equations using Harr wavelets [4]. Islameh and Aziz also proposed a method for numerically solving one-dimensional equations using wavelets [6].

In 1909, Haar was the first person to mention wavelets. Later, Jean Morelet discovered that Fourier bases were not ideal tools for underground exploration, which led to the discovery of wavelets. Mir and Mallet then laid the foundations of orthogonal wavelets and created algorithms for wavelet decomposition and reconstruction. In 1990, Morenzi and Antonie expanded wavelets to two dimensions [3]. Wavelet analysis has been used to analyze transient signals that change rapidly. It has various applications, including analyzing sound and audio signals, electrical activity in the brain, and underwater sounds. It is also used to control power plants through the NMR display of computer spectroscopic data [3, 14]. Today, Wavelets have various applications, including brain tissue separation, CT scanning in medical imaging, magnetic resonance imaging of nuclear energy, industries, agriculture, and computer software and hardware [16, 24]. Over the last two decades, there have been advancements in wavelet theory. As a result, several studies have been conducted on solving integro-differential equations using wavelet methods. For instance, in 2004, Hibbert-Taylor solved Fredholm integral equations using wavelet methods [7]. In 2012, the Legendre wavelet method was employed to solve second-type Fredholm integral equations [8]. Wavelets were also used to solve partial fractional equations. The solution for binary systems of fractional integral differential equations has been achieved by utilizing Haar and Legendre wavelets. These wavelets have been employed in solving partial fractional equations as well as binary systems of fractional integral differential equations. However, applying Haar wavelets in solving 2D fractional differential integral equations is a new and unexplored phenomenon. Therefore, we aim to utilize the Haar wavelet method to solve the two-dimensional fractional Fredholm integro-differential equations of the form,

$$D_t^{\beta} u(x,t) = f(x,t) + \int_0^1 \int_0^1 k(x,y,t,\omega) u(y,\omega) dy d\omega, \tag{1}$$

where $D_t^{\beta} u(t)$ is the fractional derivative and $u(x,t)$ be a function defined over $[0,1]\times[0,1]$, and $k(x,y,t,\omega)$ be a continuous kernel; in addition, assume $0 < \beta < 1$. This article is written as follows: The concepts of Harr wavelet and related theorems are presented in section 2. The proposed method is presented in section 3. And finally, the accuracy and efficiency of the proposed design are shown using numerical

solutions with some examples with tables and graphs in section 4.

2. Haar wavelets

Haar basis wavelet $\Psi_{i,j}(y), j \in \mathbb{N}, i \in \mathbb{Z}$ is a constant family function and an orthogonal subfamily of Hilbert space $L^2(\mathbb{R})$, a group of functions that arise from a constant function ψ called the mother wavelet. In the wavelet family, the following relations are established:

$$\Psi_{j,i}(y) = 2^{j/2}\psi(2^j y - i).$$

For the group of raging Haar wavelet in the interval $[0, 1)$ we have,

$$h_1(x) = \begin{cases} 1 & , \quad \text{for} \quad x \in [\alpha, \beta) \\ 0 & , \quad \text{elsewhere,} \end{cases} \tag{2}$$

and

$$h_i(x) = \begin{cases} 1 & , \quad \text{for} \quad x \in [\alpha, \beta) \\ 1 & , \quad \text{for} \quad x \in [\beta, \gamma) \\ 0 & , \quad \text{elsewhere,} \end{cases} , i = 2, 3, 4, \ldots,$$

where

$$\alpha_k = \frac{k}{m} \quad , \quad \beta_k = \frac{k + 0.5}{m} \quad , \quad \gamma_k = \frac{k+1}{m},$$
$$m = 2^j \quad , \quad j = 0, 1, 2, \ldots, j \quad , \quad k = 0, 1, 2, \ldots, m-1.$$

The connection between i, k, and m is given by $i = k + m + 1$. k is the transmission parameter.

In Table 1, we calculate the correct values for i, j, and k up to level $j = 3$.

Table 1. Calculation for Haar wavelet bases at $j = 3$.

k	0	0	1	0	1	2	3	0	1	2	3	4	$\cdots$	7
j	0	1	1	2	2	2	2	3	3	3	3	3	$\cdots$	3
$i = k + m + 1$	2	3	4	5	6	7	8	9	10	11	12	13	$\cdots$	16

The value of the number j denotes the maximum resolution level of the wavelet. Any specific integral function $f(x)$ in the space $[0, 1)$ can be considered as a linear combination of the grades of the Haar wavelet, such as,

$$f(x) \approx \sum_{i=1}^{2M} c_i h_i(x).$$

Here, c_i is the real coefficient in the function. The upside series concludes at confined intervals if $f(x)$ is a piece fixed [1].

According to the above explanation, we get a linear device from the following equations:

$$f(x_m) = \sum_{i=1}^{2M} c_i h_i(x_m) \quad , \quad m = 1, 2, 3, \ldots, M. \tag{3}$$

In the above text, the linear system of equations is a $2M \times 2M$, which can be calculated using the following theorem to find the unknown coefficients c_i.

Theorem 2.1 *The answer to the system (3) is as follows:*

$$c_1 = \frac{1}{2M} \sum_{m=1}^{2M} f(x_m)$$

$$c_i = \frac{1}{\mu} \left(\sum_{m=\alpha}^{\beta} f(x_m) - \sum_{m=\beta+1}^{\gamma} f(x_m) \right) \quad , \quad i = 1, 2, 3, \ldots, 2M.$$

where

$$\alpha = \mu(\lambda - 1) + 1 \quad , \quad \beta = \mu(\lambda - 1) + \frac{\mu}{2} \quad , \quad \gamma = \lambda\mu,$$

$$\mu = \frac{2M}{\theta} \quad , \quad \lambda = i - \theta \quad , \quad \theta = 2^{[\log_2(i-1)]}.$$

Proof . See [11].

Theorem 2.2 *With the variables x and y, a very good and real function $F(x, y)$ can be estimated by two dimensional wavelets in an approximate form as,*

$$F(x, y, s, t) \approx \sum_{i=1}^{2M} \sum_{j=1}^{2M} d_{i,j}(x, y) h_i(s) h_j(t).$$

Substituting the collocation point:

$$s_p = \frac{p - 0.5}{2M}, \qquad p = 1, 2, 3, \ldots, 2M,$$

and

$$t_q = \frac{q - 0.5}{2N}, \qquad q = 1, 2, 3, \ldots, 2N,$$

we get the following system of linear equations:

$$F(x, y, s_p, t_q) \approx \sum_{i=1}^{2M} \sum_{j=1}^{2N} d_{i,j} h_i(s_p) h_h(t_q), \quad p = 1, 2, 3, \ldots, 2M, \quad q = 1, 2, 3, \ldots, 2N,$$

for each value of $x, y \in [0, 1]$, the answer of this system is obtained as the following equation:

$$d_{1,1}(x, y) = \frac{1}{2M \times 2N} \sum_{p=1}^{2M} \sum_{q=1}^{2N} F(x, y, s_p, t_q),$$

$$d_{i,j}(x, y) = \frac{1}{\mu_1 \times 2N} \left(\sum_{p=\alpha_1}^{\beta_1} \sum_{q=1}^{2N} F(x, y, s_p, t_q) - \sum_{p=\beta_1}^{\gamma_1} \sum_{q=1}^{2N} F(x, y, s_p, t_q) \right),$$
$$i = 2, 3, \ldots, 2M,$$

$$d_{1,j}(x,y) = \frac{1}{\mu_2 \times 2M}\left(\sum_{p=1}^{2M}\sum_{q=\alpha_2}^{\beta_2} F(x,y,s_p,t_q) - \sum_{p=1}^{2M}\sum_{i=\beta_2+1}^{2N} F(x,y,s_p,t_q)\right),$$
$$j = 2,3,\ldots,2N,$$

$$d_{i,j}(x,y) = \frac{1}{\mu_1 \times \mu_1}\left(\sum_{p=\alpha_1}^{\beta_1}\sum_{q=1}^{\beta_2} F(x,y,s_p,t_q) - \sum_{p=\alpha_1}^{\beta_1}\sum_{i=\beta_2+1}^{\gamma_2} F(x,y,s_p,t_q)\right.$$
$$\left. - \sum_{p=\beta_1+1}^{\gamma_1}\sum_{i=\alpha_2}^{\beta_2} F(x,y,s_p,t_q) + \sum_{p=\beta_1+1}^{\gamma_1}\sum_{i=\beta_2+1}^{\gamma_2} F(x,y,s_p,t_q)\right),$$
$$i = 2,3,\ldots,2M, \quad j = 2,3,\ldots,2N.$$

Whither

$$\alpha_1 = \mu_1(\lambda_1 - 1) + 1 \quad , \quad \beta_1 = \mu_1(\lambda_1 - 1) + \frac{\mu_1}{2} \quad , \quad \gamma_1 = \lambda_1\mu_1, \tag{4}$$
$$\mu_1 = \frac{2M}{\theta_1} \quad , \quad \lambda_1 = i - \theta_1 \quad , \quad \theta_1 = 2^{[\log_2(i-1)]},$$

and also

$$\alpha_2 = \mu_2(\lambda_2 - 1) + 1 \quad , \quad \beta_1 = \mu_2(\lambda_2 - 1) + \frac{\mu_2}{2} \quad , \quad \gamma_2 = \lambda_2\mu_2, \tag{5}$$
$$\mu_2 = \frac{2M}{\theta_2} \quad , \quad \lambda_2 = i - \theta_2 \quad , \quad \theta_2 = 2^{[\log_2(i-1)]}.$$

Proof . [2].

Consider the parameters t, y, x, and s from the function $F(x, y, s, t)$. Let's assumption that the function $F(x, y, s, t)$ is estimated by used to of a 2- dimensional Haar wavelet as follows:

$$F(x,y,s,t) \approx \sum_{i=1}^{2M}\sum_{j=1}^{2N} d_{i,j}(x,y)h_i(s)h_j(t).$$

We achieved the consequent system of linear equations.

Corollary 2.1 Consider $F(x, y)$ that includes two parameters y and x, which is estimated via the Haar wavelet access presented in Equation (1). Further suppose such $F(x, y)$ at the points $(x_m, y_n), n = 1, 2, , 2N, m = 1, 2, ..., 2M$. Therefore, at any point of the domain of the function $F(x, y)$, its approximate value can be

obtained as tracks:

$$
\begin{aligned}
F(x,y) = {} & \frac{1}{2M \times 2N} \sum_{p=1}^{2M} \sum_{q=1}^{2N} F(x_m, y_n) h_1(x) h_1(y) \\
& + \sum_{i=1}^{2M} \frac{1}{\mu_1 \times 2N} \left(\sum_{p=\alpha_1}^{\beta_1} \sum_{q=1}^{2N} F(x_m, y_n) - \sum_{p=\beta_1}^{\gamma_1} \sum_{q=1}^{2N} F(x_m, y_n) \right) h_i(x) h_1(y) \\
& + \sum_{i=1}^{2N} \frac{1}{\mu_2 \times 2M} \left(\sum_{p=1}^{2M} \sum_{q=\alpha_2}^{\beta_2} F(x_m, y_n) - \sum_{p=1}^{2M} \sum_{q=\beta_2+1}^{\gamma_2} F(x_m, y_n) \right) h_1(x) h_j(y) \\
& + \sum_{i=1}^{2M} \sum_{j=1}^{2N} \frac{1}{\mu_1 \times \mu_2} \left(\sum_{p=\alpha_1}^{\beta_1} \sum_{q=\alpha_2}^{\beta_2} F(x_m, y_n) - \sum_{p=\alpha_1}^{\beta_1} \sum_{q=\beta_2+1}^{\gamma_2} F(x_m, y_n) \right. \\
& \left. - \sum_{p=\beta_1+1}^{\gamma_1} \sum_{q=\alpha_2}^{\beta_2} F(x_m, y_n) + \sum_{p=\beta_1+1}^{\gamma_1} \sum_{q=\beta_2+1}^{\gamma_2} F(x_m, y_n) \right) h_i(x) h_j(y),
\end{aligned}
$$

where $\alpha_1, \beta_1, \gamma_1$ and μ_1 are defined as in Eq. (4) and $\alpha_2, \beta_2, \gamma_3$ and μ_2 are defined as in Eq. (5)

3. Solution method

When dealing with both $u(x)$ and its derivative $u'(x)$ in differential integral equations of Haar wavelet in relation (2) is introduced as follows:

$$
q_i = \int_0^x h_i dx = \begin{cases} x - \frac{k}{2^j} & , \frac{k}{2^j} \leqslant x \leqslant \frac{k+0.5}{2^j} \\ \frac{k+1}{2^j} - x & , \frac{k+0.5}{2^j} \leqslant x \leqslant \frac{k+1}{2^j} \\ 0 & , \text{elsewhere.} \end{cases} \tag{6}
$$

Which if approximated $u'(x) \approx \sum_{i=1}^{2^{J+1}} b_i h_i(x)$ as a result $u(x) - u(0) \approx \sum_{i=1}^{2^{J+1}} b_i h_i(x)$.

First, we detect the level of clarity j to proximate $U(x,t)$, then we assume,

$$
\frac{\partial}{\partial t} U(x,t) \approx \sum_{i=1}^{2^{J+1}} \sum_{j=1}^{2^{J+1}} b_{ij} h_i(x) h_j(t). \tag{7}
$$

Wherever $\{b_{ij}\}$ are to be found. From the initial condition $u(x,0) = 0$ and the composition t in $[0,t]$, can be written,

$$
U(x,t) \approx \sum_{i=1}^{2^{J+1}} \sum_{j=1}^{2^{J+1}} b_{ij} h_i(x) q(t).
$$

The following integral expression can be written as a result,

$$\int_0^1 \int_0^1 K(x,t,y,\omega)U(y,\omega)dyd\omega \approx \sum_{i=1}^{2^{J+1}} \sum_{j=1}^{2^{J+1}} b_{ij} \int_0^1 \int_0^1 K(x,t,y,\omega)h_i q_j(\omega)dyd\omega.$$

To evaluate the phrase $D_t^\beta u(x,t)$, we connection relation (7) into the $D_t^\beta u(x,t)$, obtained,

$$\frac{1}{\zeta(1-\beta)} \sum_{i=1}^{2^{J+1}} \sum_{j=1}^{2^{J+1}} b_{ij} h_i(x) \int_0^t h_j(\omega)(t-\omega)^{-\beta} d\omega$$
$$= f(x,t) + \sum_{i=1}^{2^{J+1}} \sum_{j=1}^{2^{J+1}} b_{ij} \int_0^1 \int_0^1 k(x,t,y,\omega)h_i(y)q_j(\omega)dyd\omega.$$

With the help of nodes with equal distance $t_n = \frac{n}{2^{J+1}}$ and $x_m = \frac{m-0.5}{2^{J+1}}$ to create the system,

$$\frac{1}{\zeta(1-\beta)} \sum_{i=1}^{2^{J+1}} \sum_{j=1}^{2^{J+1}} b_{ij} h_i\left(x_m\right) \int_0^{t_n} h_j(\omega)\left(t_n-\omega\right)^{-\beta} d\omega$$
$$= f\left(x_m,t_n\right) + \sum_{i=1}^{2^{J+1}} \sum_{j=1}^{2^{J+1}} b_{ij} \int_0^1 \int_0^1 k\left(x_m,t_n,y,\omega\right) h_i(y)q_j(\omega)dyd\omega,$$

where $\mathrm{n},\mathrm{m} = 1,2,3,\ldots,2^{J+1}$.

By solving the system of equations $2^{J+1} \times 2^{J+1}$ in the above relation, the value of wavelet coefficients b_{ij} is obtained.

4. Numerical tests

In this section, we demonstrate the effectiveness, precision, application, and efficiency of the proposed method by providing several examples of a single weak PIDE. To do this, we utilize the definition of absolute error, denoted as e_M. It is defined as,

$$e_M(x,y) = \left|u(x,y) - u_M(x,y)\right|.$$

Here, $u(x,y)$ shows the approximate answer, and $u(x,y)$ shows the exact result achieved using the suggested method.

Let us consider the mesh nodes on the square and the asymptotic spread powers of the step size h as,

$$x_m = \frac{m-0.5}{2M}, \quad m = 1,2,3,\ldots,2M,$$
$$y_n = \frac{n-0.5}{2N}, \quad n = 1,2,3,\ldots,2N, \quad 0 \leqslant x,y \leqslant 1,$$
$$G(h) - G(0) = \beta h^k + o(h^s), \quad 0 < k < s. \tag{8}$$

Here $G(0)$ is the unknown correct value, $G(h)$ means the quantity achieved with any numeric procedure with level range h, k is the theoretical order of exactness, and β is an unknown fixed independent of h.

Mean two numerical solutions established on the nested grid as follows,

$$G_{i-1} = G\left(h_{i-1}\right) \quad , \quad G_i = G\left(h_i\right).$$

Applying (8) for these explanations, the following equality,

$$\begin{aligned} G_{i-1} - G(0) &= \beta h_{i-1}^k + O(h_{i-1}^s) \\ G_i - G(0) &= \beta h_i^k + O\left(h_i^s\right). \end{aligned} \tag{9}$$

The error value can be obtained by combining these two relations. So, the value becomes an error as,

$$G(0) - G_i = \frac{G_i - G_{i-1}}{2^k - 1} - O\left(h_i^s\right). \tag{10}$$

Or another approximation of the value $G(0)$ as,

$$E_i = G_i + \frac{G_i - G_{i-1}}{2^k - 1} = G(0) - O\left(h_i^s\right). \tag{11}$$

This simplified formula is known as the Richardson analogy formula. In essence, the approximate solutions E_i have more error than h of G_i. Therefore, if the numerical solutions for two grids and the theoretical order of accuracy k are known from the numerical method, as a simple analogical formula (11), it removes the preceding term from the error of the expansion equation (8) and leads us to an acceptable solution [11].

In this study, we employed Richardson's extrapolation method to assess the error in finite difference methods for various mathematical issues.

From solving the real value of $G(0)$ in (9), provide a simple method for assessing the convergence rate of the numerical approach as,

$$\frac{G_{i-1} - G(0)}{G_i - G(0)} = 2^k + \mathrm{O}\left(h_i^{s-k}\right) = \frac{\log\left(\frac{G_{i-1} - G(0)}{G_i - G(0)}\right)}{\log 2}. \tag{12}$$

It is possible to guess and estimate the accuracy of visionary content using three paths on a series of nested networks,

$$G_{i-2}, G_{i-1}, G_i, \frac{h_{i-2}}{h_{i-1}} = \frac{h_{i-1}}{h_i} = 2.$$

The beneath relation can be achieved from three relationships a like to parity (12),

$$\omega_i = \frac{G_{i-2} - G_{i-1}}{G_{i-1} - G_i} = 2^k + \mathrm{O}\left(h_i^{s-k}\right). \tag{13}$$

With the help of relationship (18), the order of accuracy k can be evaluated and

specified [16],

$$k \cong k_i = \frac{\log(\omega_i)}{\log 2}. \tag{14}$$

Here, k_i is an amount of discovered degree of precision, and relation (14) grants the pilot procedure for determinative or evident relation (14) can be used only for $\omega_i > 0$.

Further, the following formula can be applied to evaluate the order of convergence for the advanced value E_i.

$$s \cong s_i = \frac{\log\left(\frac{E_{i-2}-E_{i-1}}{E_{i-1}-E_i}\right)}{\log 2}. \tag{15}$$

Example 4.1 Notice the following two-dimensional fractional integro-differential equation:

$$\begin{cases} D_t^{\frac{5}{2}} u(x,t) = -2\pi^{\frac{5}{2}}\left(-6+\pi^2\right) + 12\sqrt{t}\sin(\pi x)\displaystyle\int_0^1\int_0^1 ye^{\omega}u(y,\omega)td\omega dy, \\ \\ u(x,0) = 0. \end{cases} \tag{16}$$

The exact solution of Equation (16) is $u(x,t) = \sqrt{\pi}t^3\sin(\pi x)$.

We use the Haar wavelet method the level of resolution $J = 4$. The following discrete system is given by the proposed method.

$$\sum_{i=1}^{32}\sum_{j=1}^{32} b_{ij}h_i(x_m)h_j(t_n) = \frac{16}{15}\pi^2\left(6-\pi^2\right)(t_n)^{\frac{5}{2}} + \sqrt{\pi}(t_n)^3\sin(\pi x_m) + \frac{8\pi^5\sqrt{\pi}}{15}\sum_{i=1}^{32}\sum_{j=1}^{32} b_{ij}(t_n)^{\frac{5}{2}}q_i\int_0^1\sin(\pi t)h_j(t)dt,$$

by approximate solution,

$$u(x,t) \approx \sum_{i=1}^{32}\sum_{j=1}^{32} b_{ij}h_i(x_m)h_j(t_n).$$

Table 2.. Approximate, absolute error and exact for distinct of t_n and x_m in example 4.1 with $J = 4$.

x_m	t_n	approximate value	exact value	absolute error
0.734375		0.00171454	0.0017183	3.83569×10^{-6}
0.484375		0.00231252	0.00231636	3.83569×10^{-6}
0.359375		0.00209265	0.00209649	3.83569×10^{-6}
0.234375	0.109375	0.00155361	0.00155745	3.83569×10^{-6}
0.109375		0.000777463	0.000781299	3.83569×10^{-6}
0.046875		0.00033645	0.00034029	3.83569×10^{-6}
0.015625		0.00109392	0.0011971	2.57826×10^{-5}
0.046875		0.00332255	0.00334834	2.57826×10^{-5}
0.234375	0.234375	0.015299	0.0153247	2.57826×10^{-5}
0.484375		0.0227664	0.0227922	2.57826×10^{-5}
0.734375		0.0168825	0.0169082	2.57826×10^{-5}
0.984375		0.00109392	0.00111971	2.57826×10^{-5}

The chart approximate and exact solution for example 4.1. with purpose $J = 4$.

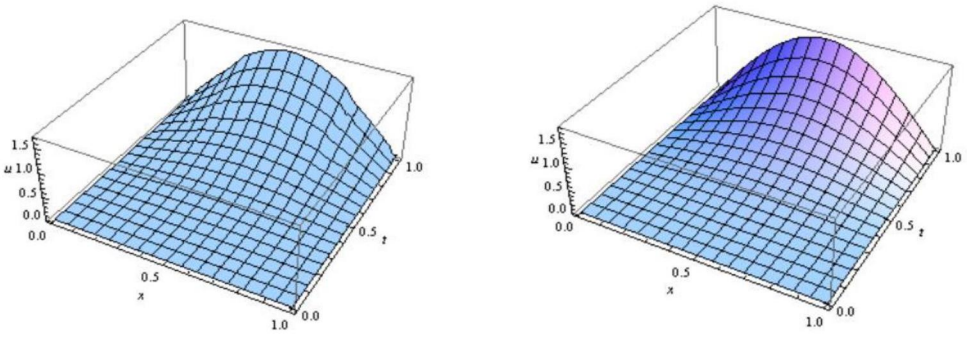

Figure 1. The approximate (to the left) and the exact (to the right) solutions for example 4.1 with $J = 4$ using Haar wavelet method.

Example 4.2 Notice the following 2-D linear fractional integro-differntial equation:

$$\begin{cases} D_t^{0.5}u(x,t) = \dfrac{\sqrt{\pi}}{2}e^x - \dfrac{2(e-1)}{3} + \displaystyle\int_0^1 \int_0^1 u(y,\omega)td\omega dy, \\ \\ u(x,0) = 0. \end{cases} \tag{17}$$

The precise solution of Equation (17) is $u(x,t) = \sqrt{t}e^x$. We solve this example differently using the Haar wavelet.

To estimate the value of $D_t^{0.5}u(x,t)$, we use,

$$\frac{\partial}{\partial t}u(x,t) \approx \sum_{i=1}^{32}\sum_{j=1}^{32} b_{ij}h_j(x)h_j(t). \tag{18}$$

Considering the condition $u(x,0) = 0$, to find that,

$$u(x,t) \approx \sum_{i=1}^{32}\sum_{j=1}^{32} b_{ij}h_i(x)q_j(t). \tag{19}$$

By using the estimates in (18), (19) and nods $t_n = \frac{n-0.5}{32}$ and $x_m = \frac{m-0.5}{32}$, following system is obtained,

$$\frac{1}{\sqrt{\pi}} \sum_{i=1}^{32} \sum_{j=1}^{32} b_{ij} h_i(x) \int_0^{t_n} h_j(\omega) \left(t_n - \omega\right)^{-0.5} d\omega$$

$$= \sum_{j=1}^{32} b_{ij} t_n q_i(1) s_j(1) + \frac{\sqrt{\pi}}{2} e^{x_m} - \frac{2(e-1)t_n}{3},$$

where,

$$s_j(x) = \int_0^x q_j(y) dy \quad \text{and} \quad n, m = 1, 2, 3, \ldots, 32.$$

Table 3. Approximate, absolute error and exact for distinct of t_n and x_m in example 4.2 with $J = 4$.

x_m	t_n	approximate value	exact value	absolute error
0.984375		1.86251	1.86228	2.37762×10^{-4}
0.4734375		1.45053	1.45029	2.38002×10^{-4}
0.48437		1.12943	1.12967	2.38189×10^{-4}
0.234375	0.484375	0.879551	0.879789	2.38335×10^{-4}
0.109375		0.776173	0.776411	2.38395×10^{-4}
0.015625		0.706692	0.70693	2.38435×10^{-4}
0.984375		1.29551	1.29558	7.13023×10^{-5}
0.734375		1.00893	1.009	7.32756×10^{-5}
0.234375	0.234375	0.611913	0.611989	7.60092×10^{-5}
0.484375		0.785734	0.785809	7.48123×10^{-5}
0.109375		0.540002	0.540078	7.65043×10^{-5}
0.015625		0.49157	0.491747	7.68371×10^{-5}

The chart approximate and exact solution for example 4.2 with purpose $J = 4$.

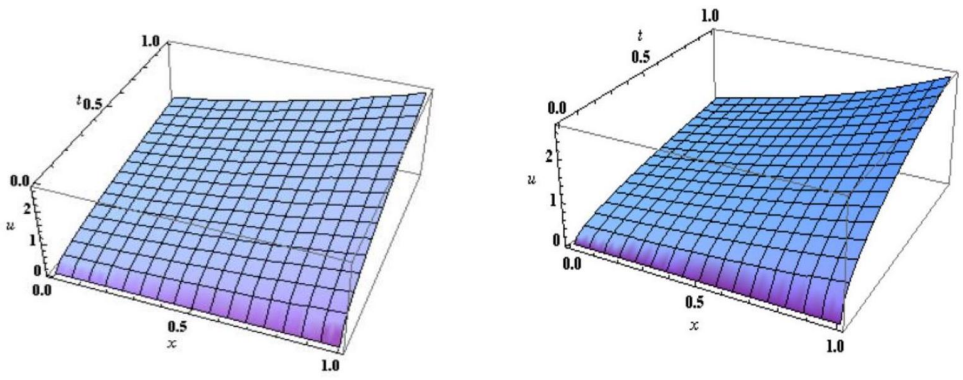

Figure2. The approximate (to the left) and the exact (to the right) solutions for example 4.2 with $J = 4$ using Haar wavelet method.

Example 4.3 Notice the following 2-D linear fractional integro-differntial equation:

$$\begin{cases} D_t^{0.5}u(x,t) = 8t^{\frac{2}{3}}\frac{\sin(\pi x)}{\pi x} + 6(2-e) + \pi\sqrt{\pi}\int_0^1\int_0^1 ye^{\omega}u(y,\omega)dyd\omega, \\ u(x,0) = 0. \end{cases} \tag{20}$$

The accurate solution of relation (20) is $u(x,y) = 3\sqrt{\pi}t^2\frac{\sin\pi x}{\pi x}$.
We use Haar wavelet method at $J = 4$.

$$\frac{1}{\sqrt{\pi}}\sum_{i=1}^{32}\sum_{j=1}^{32} b_{ij}h_i(x_m)\int_0^{t_n} h_j(\omega)(t_n-\omega)^{-0.5}\,d\omega$$

$$= 8t_n^{\frac{3}{2}}\frac{\sin\pi x}{\pi x}x_m + 6(2-\mathrm{e}) + \pi\sqrt{\pi}\sum_{i=1}^{32}\sum_{j=1}^{32} b_{ij}\left(\int_0^1 q_j(\omega)e^{\omega}d\omega\right)\left(\int_0^1 yh_i(y)dy\right),$$

for $m,n = 1,2,3,\ldots,32$, and $t_n = \frac{n-0.5}{32}, x_m = \frac{m-0.5}{32}$.

Table 4. Approximate, absolute error and exact for distinct of t_n and x_m in example 4.3 with $J = 4$.

x_m	t_n	approximate value	exact value	absolute error
0.984375		0.0054642	0.00463451	8.29692×10^{-4}
0.4734375		0.0941176	0.0938081	3.67342×10^{-4}
0.484375		0.191455	0.191718	2.63576×10^{-4}
0.359375	0.234375	0.233365	0.233875	5.0993×10^{-4}
0.234375		0.265705	0.266405	7.00023×10^{-4}
0.109375		0.285561	0286377	8.16738×10^{-4}
0.984375		0.08334443	0.0817527	1.69153×10^{-3}
0.734375		1.65523	1.65473	4.53913×10^{-4}
0.484375		3.38101	3.38101	9.04961×10^{-4}
0.359375	0.984375	4.12407	4.12556	1.49005×10^{-3}
0.234375		5.04948	5.0517	2.21871×10^{-3}
0.015625		5.14813	5.15042	2.29639×10^{-3}

The chart approximate and exact solution for example 4.3 with purpose $J = 4$.

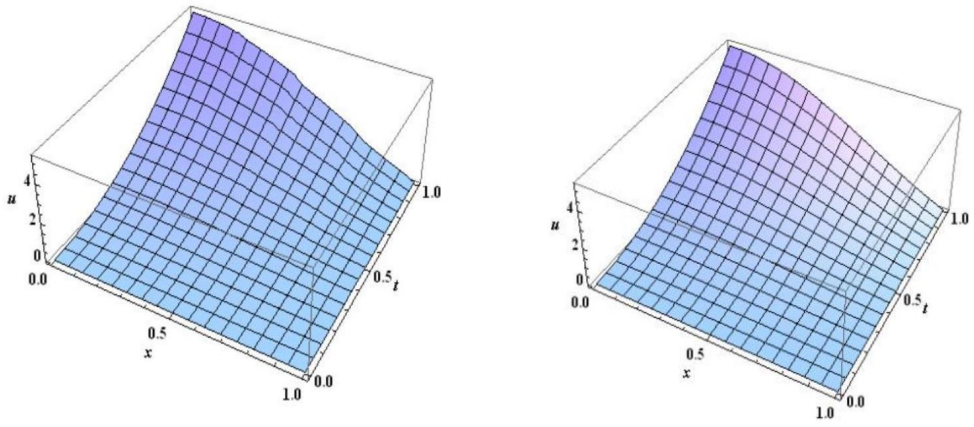

Figure 3. The approximate (to the left) and the exact (to the right) solutions for example 4.3 with $J = 4$ using Haar wavelet method.

5. Conclusions

In this article, Fredholm's two-dimensional partial differential integral equations were solved using the Haar wavelet. The proposed technique results in high accuracy. Theoretical discussions about convergence and approximation error estimation have also been presented, and the experimental results obtained from some illustrative examples prove this issue well. Finally, the reliability and simplicity of the method are shown using numerical examples, graphs, and tables.

Funding

This research was conducted without any external funding .

Acknowledgments

The authors express their gratitude to the editor and the anonymous referees for their comprehensive review and valuable comments.

Conflict of interest

The authors declare that there are no competing interests or conflicts of interest regarding the publication of this article.

References

[1] A. Babaaghaie, K. Maleknejad, Numerical solutions of nonlinear two-dimensional partial Volterra integro-differential equations by Haar wavelet. **317** (2017) 643-651.
[2] I. Aziz, S.Islam, F. Khan, A new method based on Haar wavelet for the numerical solution of two-dimensional nonlinear integral equations, J. Comput. Appl. Math. **272** (2014) 70-80.
[3] D. Lokenath, Wavelet Transforms Their Applications, *Birkhauser*, 2001 pp. 12.
[4] S. Yasmeen, and R. Amin, Higher-order Haar wavelet method for solution of fourth-order integro-differential equations. Journal of Computational Science, **81** (2024) 102394.
[5] P. Rahimkhani, Y. Ordokhani, E. Babolian, A new operational matrix based on Bernoulli wavelets for solving fractional delay differential equations, Numer. Algorithms vol. **74 (1)** (2017) 223-245.
[6] I.Aziz, M.Fayyaz, A new approach for numerical solution of integro-differential equations via Haar wavelets Int. J. Comput. Math. **90**, (2013) 1971-1989.
[7] E. Babolian, K. Maleknejad, M. Roodaki, H. Almasieh, Two dimensional triangular functions and their applications to nonlinear 2d VolterraFredholm equations, Math. Appl. **60** (2010) 1711-1722.
[8] K. Malenknejad, Z. JafariBehbahani, Application of two-dimensional triangular functions for solving nonlinear class of mixed Volterra-Fredholm integral equations, Math. Comput. Modelling **55** (2012) 1833-1844.
[9] A.A. Khajehnasiri, R. Ezzati and A. Jafari Shaerlar, Walsh functions and their applications to solving nonlinea fractional Volterra integro-differential equation, Int. J. Nonlinear Anal. Appl. **12** (2021) 1577-1589.
[10] A.A. Khajehnasiri and R. Ezzati, Boubaker polynomials and their applications for solving fractional two dimensional nonlinear partial integro-differential Volterra integral equations, Comput. Appl. Math. **41** (2022) 46-56.
[11] I. Aziz, Siraj-ul-Islam, New algorithms for numerical solution of nonlinear Fredholm and Volterra integral equations using Haar wavelets, J. Comput.Appl. Math. **239** (2013) 333-345.
[12] F. Mirzaee, S. Alipour, Approximate solution of nonlinear quadratic integral equations of fractional order via piecewise linear functions, J. Comput. Appl. Math. vol. **331** (2018) 217-227.
[13] K.D. Dwivedi and J. Singh, Numerical solution of two-dimensional fractional-order reaction advection sub diffusion equation with finite-difference Fibonacci collocation method, Math. Comput. Simul. **270** (2021) 38-50.
[14] I. Zamanpour and R. Ezzati, Operational matrix method for solving fractional weakly singular 2D partial Volterra integral equations, J. Comput. Appl. Math. **419** (2023) 1-19.
[15] S. Sabermahani, Y. Ordokhani and S.A. Yousefi, Numerical scheme for solving singular fractional partial integrodifferential equation via orthonormal Bernoulli polynomials, Int. J. Numer. Mode. **351** (2019 73-88.

[16] J. Majak, B. S. Shvartsman, M. Kirs, M. Pohlak, and H. Herranen, Convergence theorem for the Haar wavelet based discretization method, Comp. Struct. **126** (2015) 227-232.
[17] I. Zamanpour and R. Ezzati, Operational matrix method for solving fractional weakly singular 2D partial Volterra integral equations, J. Comput. Appl. Math. **419** (2023) 1-19.
[18] M. Irfan and F.A. Shah, Fibonacci wavelet method for solving the time-fractional bioheat transfer model, Optik **95** (2021) 644-651.
[19] I. Zamanpour and R.Ezzati, solving fractional two-dimentional nonlinear weakly singular partial integro-differential equation by using Fibonacci polynomials, Int J. Nanlinear. Apple. **14** (2023) 11-24.
[20] Suthar, D. L., Kumar, D., and Habenom, H. Solutions of fractional Kinetic equation associated with the generalized multiindex Bessel function via Laplace transform. Differential Equations and Dynamical Systems, (2019) 1-14.
[21] V.Singh, and D.N. Pandey, Multi-term Time-Fractional Stochastic Differential Equations with Non-Lipschitz Coefficients. Differential Equations and Dynamical Systems, **30 (1)** (2022) 197-209.
[22] R.Sevinik Adigzel, U. Aksoy, E.Karapinar, and I.M. Erhan, On the solution of a boundary value problem associated with a fractional differential equation. Mathematical Methods in the Applied Sciences, **47 (13)** (2024) 10928-10939.
[23] S.M. Sivalingam, P.Kumar, and Govindaraj, A neural networks-based numerical method for the generalized Caputo-type fractional differential equations. Mathematics and Computers in Simulation, **213** (2023) 302-323.
[24] M.T.Kartal, O. Depren, and F. Ayhan, Uncovering Displacement between Nuclear and Renewable Electricity Generation for G7 Countries by Novel Wavelet-Based Methods. International Journal of Sustainable Development & World Ecology, (2024) 1-18.